Article

Geochemical Behavior of Lanthanides and Actinides in an Old Uranium Mine, Portugal

Andrés Cardenas [1,*] , Maria I. Dias [1,2], Catarina Diamantino [3] , Edgar Carvalho [3], Dulce Russo [1,2] and Rosa Marques [1,2]

1   Center for Nuclear Sciences and Technologies (C2TN), Instituto Superior Técnico, Universidade de Lisboa, EN 10 (km 139.7), 2695-066 Bobadela, Portugal; isadias@ctn.tecnico.ulisboa.pt (M.I.D.); dulcef@ctn.tecnico.ulisboa.pt (D.R.); rmarques@ctn.tecnico.ulisboa.pt (R.M.)
2   Department of Nuclear Sciences and Engineering (DECN), Instituto Superior Técnico, Universidade de Lisboa, EN 10 (km 139.7), 2695-066 Bobadela, Portugal
3   EDM—Empresa de Desenvolvimento Mineiro S.A., Rua Sampaio e Pina, 1-3° Dt°, 1070-248 Lisboa, Portugal; catarina.diamantino@edm.pt (C.D.); edgar.carvalho@edm.pt (E.C.)
*   Correspondence: andres.nino@ctn.tecnico.ulisboa.pt

Abstract: New insights about the geochemical behavior of actinides and lanthanides in an old uranium mine are provided for the first time in this work. Fifteen samples (water, soil, and sediments) were collected inside and outside the Quinta do Bispo old mine (Portugal) in order to better understand the lanthanide and actinide behavior in the soil–water system. The chemical and mineralogical composition was obtained via ICP-MS, INAA, and XRD. The water sample from the open pit exhibits a higher U and REE dissolved concentration when compared to the other water samples. A positive Eu anomaly is found in this sample. The soil samples collected inside the mine area, including mine waste rocks and the minesoils surrounding the open pit, show uranium mineral phases, higher U contents, an enrichment of LREE relative to HREE, and a lower Th/U. This heterogeneity may be due to the open pit extraction and ore processes, as well as the percolation and water infiltration through the waste rock piles. Soils from outside the mine area have a similar mineralogical and chemical composition, despite their different geological context, which could be related to the influence of the granitic geological unit during the alluvial unit deposition. The sediments have similar REE patterns, negative Eu anomaly, and a high $(La/Yb)_N$.

Keywords: rare earth elements; uranium mine; central Portugal; lanthanides and actinides; geochemistry

1. Introduction

Rare earth elements (REE) include the lanthanide series elements (La, Ce, Pr, Nd, Pm, Sm, Eu, Gd, Tb, Dy, Ho, Er, Tm, Yb, and Lu) plus Sc and Y, as defined by the International Union of Pure and Applied Chemistry (IUPAC). Actinides correspond to the series of elements beginning with actinium and include thorium, protactinium, uranium, and the trans uranium elements through the element lawrencium. Actinides are heavy due to their large atomic mass, and one of their most important properties is that they are radioactive in nature. Some similarities can be found between lanthanides and actinides, such as the dominant oxidation state +3. In the case of lanthanides, Eu can be found in a divalent state under reducing conditions, and Ce in the tetravalent state under oxidizing conditions [1].

According to the British Geological Survey [2], REE deposits can be broadly divided into: (1) primary deposits associated with igneous and hydrothermal processes (e.g., carbonatite, alkaline igneous rocks); and (2) secondary deposits concentrated by sedimentary processes and weathering (e.g., marine, and alluvial placers, ion-adsorption clays, laterites). Currently, the world reserves of REE are found mainly in China, Brazil, Vietnam, Russia, and India [3]. REEs are found in a wide range of minerals, including silicates, carbonates, oxides, and phosphates, but they do not fit into most mineral structures and can only be

found in a few geological environments. The principal economic sources of REE minerals are bastnaesite, monazite, and loparite and the lateritic ion-adsorption clays [4]. However, their origin and behavior in the Earth's mantle and crust have been well characterized, many uncertainties in our current understanding and modeling are related to the lack of studies on the REE anthropogenic sources (e.g., mining and mining waste, recycling wastes, gasoil, oil sands, etc.) [5].

Regarding actinides, uranium exploitation creates significant amounts of mining wastes and radioactive waste tailing. These tailings created long- and short-term environmental impacts (USA, Germany, France, and Portugal) [6], and may promote the enrichment of some elements in waters, soils, and agricultural products. For this reason, during the last quart of the 20th century the governments, such as the USA and West Europe, created legislation for environmental and health protection, and some mine remediation and rehabilitation were initiated in the industrial legacy paid by public funds [6].

Several studies have been performed with uranium mine residues around the world. In Canada, the uranium mine tailing from Athabasca Basin (Saskatchewan) was identified as a good secondary source of REE [7,8]. In Brazil, the REE potential in AMD produced by uranium waste was evaluated (deposit located in the Mesozoic alkaline complex of Poços de Caldas, Southwestern of Minas Gerais state) [9], a study perfomed on the water samples with high contents of trace metals and Y from an acidic lake of the same Brazilian mine [10], and the evaluation of the downflow fixed-structured bed biological reactor (DFSBR) in the biological treatment of the AMD were carried out.

In Portugal, several uranium mines were exploited during the 20th century for radium and uranium production. These mining and milling activities originated about 13 million tons of solid wastes dumped at several sites in the center–north region of the country [11]. The uranium production ceased in 2001, and an agreement between the Empresa de Desenvolvimento Mineiro S.A. (EDM) and the Portuguese state was established under an exclusive concession contract and approved by the Decree-Law n. ° 198-A/2001, for the environmental remediation of 175 abandoned old mines, then updated to 199 [12,13]. Several studies have been performed in the center–north of Portugal on different types of mine areas (uranium and polymetallic mines), such as the study of the uranium mineral alteration from a Portuguese Variscan peraluminous granite [14], some works concerning the trace element distribution, especially U in the aplite [15,16], and the identification of the most suitable material for REE recovery [17]. In these mining areas, studies regarding the pollution patterns and environmental impact caused by the mine exploitation were performed. In the abandoned Mondego Sul uranium mine [18], other studies were carried out, including the geochemical characterization of water, soil, and stream sediments, the identification and characterization of AMD sources, and the impact on the water quality [19]. At the Cunha Baixa mine, the effect of using contaminated water for irrigation in agriculture soils [20] was evaluated. A radiological assessment in the soil and water samples was also performed around old uranium and radium mines in the Viseu and Guarda areas [6,11]. Complementary research comprises geophysical methods and geological outcrop studies in several geological and hydrogeological critical areas of old open pits of Portugal mainland to identify potential groundwater circulation and the spread of contaminated waters [21].

Considering the importance of the former research studies related with old uranium mines, this work was performed in the Quinta do Bispo old uranium mine, where the first phase of the environmental remediation works started in 2020, including the demolition of existing settling ponds and monitoring building, and the construction of a basin and cell for the temporary deposit of waste. In addition, intervention works such as fencing, drainage, and pumping were carried out in the open pit. Additionally, a new mine water treatment facility using an active treatment system operation [22] was initiated. This mine has also been the subject of several studies, namely the lithological modeling with the weathering levels and simulation of fracture density obtaining a 3D model of transmissivity [23]. However, this mine has a lack of information, particularly regarding the geochemical characterization of uranium mining wastes, namely the REE, U, and Th behavior. This is

crucial to better improve the management of the surrounding area. The general efforts of this study are concentrated on the importance of knowing geochemical processes which have particular importance in old mining environments. In this way, the specific objectives of the present work comprise the first geochemical approach applied to the old uranium mine area of Quinta do Bispo including: (i) the study of the mineralogical and chemical composition of soils, and sediments inside and outside the mine area; and (ii) the study of the REE, Th, and U geochemical processes in the water, soil, and sediment samples from inside and outside of the mine area.

2. Geological Setting

The Quinta do Bispo old uranium mine is located in the Viseu district, central Portugal [24–26]. This ore bed was discovered in 1957 and the exploration by the open pit started in 1979 and lasted for 8 years. This exploration occupied a surface area of 158,000 m^2 and had a depth of 75 m [26]. In the Quinta do Bispo mine, besides mining and milling, chemical processes for uranium extraction took place in two different areas. Initially, the ore treatment was delivered via heap-leaching in Urgeiriça during the 1979–1987 period. Then, the new facility for ionic exchange was installed in the Quinta do Bispo mine due to the significant concentration of uranium in the water accumulated in the old open pit [27]. Regarding the geological context in the mining area (Figure 1), the main geological unit is the two mica granites, medium-to-coarse-grained (medium granite). A tendency toward profiroidism is frequent, particularly near the areas of contact with mineralized structures and enclaves of the mica schists. The outcrops of meta-sediments of the Schist Greywacke Complex also occur with strong contact metamorphism and the occurrence of migmatites. The granularity of these granites may vary in depth, which presupposes a more peripheral location. At the border of a batholitic structure, the materials are of a granitic nature and have been subjected to the action of a very fluid magma that had intruded laterally into the formations [24,26]. The mineralization comprises autunite and torbenite. Black uranium minerals occur in meta-sediments and granites. The uraniferous region of Cunha Baixa and Quinta do Bispo show three types of the granites: biotitic monzonite and coarse-grained porphyroid granite (coarse granite); monzonite two-mica medium-grain porphyroid tendency granite (medium granite); monzonite, muscovite and biotitic porphyroid and medium-to-fine-grain granite (fine granite) [26].
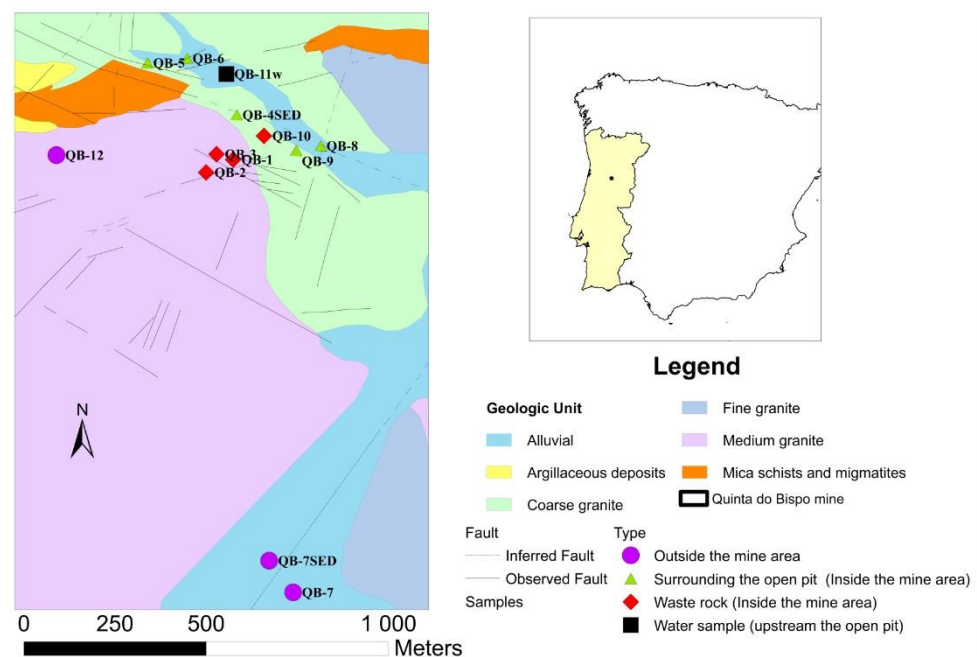
Figure 1. Geological context of the Quinta do Bispo (Portugal) old uranium mine area, with the sampling point locations (QB) (adapted from [26]).

Moreover, in the north and northwest part of the Quinta do Bispo old mine, the open pit is composed of two micas, a medium-grain porphyroid granite (medium granite) with some pegmatitic interleaving. This granite, when intersected by the most important faults, particularly from the WNW-ESSE to NW-SE direction, is quite sericite and clayey. At the south, southwest, and west of the open pit, a medium-grained granite, predominantly biotitic, shows slight chloritization effects is the dominant geology. In certain areas, the texture may have porphyroid characteristics due to the presence of tabular feldspar phenocrystals [26]. The uraniferous structures are composed of brecciated quartz veins and dissemination pockets. The main ore minerals are autunite and torbernite. Manganese oxides, pyrite, and arsenopyrite are also present in the mineralogical association [26].

3. Materials and Methods

The sampling campaign was performed in the Quinta do Bispo old uranium mine (Viseu, Portugal) in November 2020, including three water samples, ten soil samples (at a 10–20 cm depth), and two sediment samples (Figure 1).

The sampling points were selected taking into consideration different locations in the mining and surrounding areas (affected by the mining activity inside the old mine: waste rock piles, surrounding the open pit; and outside the old mine unaffected by the mining activity), also considering the geological context.

Two water samples were collected inside the old mine area, with one sample in the open pit (QB-4w) and the other collected in a flooded natural lagoon located upstream of the open pit (QB-11w). This lagoon receives the contribution from surface runoff water and possibly also from groundwater seepage, and is named a groundwater sample. The third sample was collected in the Castelo River (QB-7w), downstream the open pit (outside the mine area).

The soil samples were collected inside and outside the old mine area: (i) inside, four samples were collected in the waste rock piles (QB-1, QB-2, QB-3, and QB-10), and four minesoil samples surrounding the open pit (QB-5, QB-6, QB-8, and QB-9); and (ii) outside two samples were collected outside the old mine area (QB-7 and QB-12). It should be noted that sample QB-8 was collected in an old water line within the mine area, in the middle of the two geological faults.

Regarding the sediment samples, one was collected in the open pit (QB-4 SED) and the other was collected in Castelo River (QB-7 SED).

The total water samples (100 mL) were collected with plastic syringes and not filtered. Then, the dissolved water samples (30 mL) were filtered (<0.45 μm) in the field, and both samples were acidified with nitric acid (HNO_3) until the pH was below 2, and stored in cleaned plastic bottles. In situ parameters (pH, temperature, oxidation–reduction potential (ORP), oxygen dissolved (OD), electroconductivity (EC), total dissolved solid (TDS)) were measured in the water samples by the means of Aquaread AP-2000-D from Eijkelkamp. The samples were then analyzed for the determination of REE and other trace elements (Th and U) via inductively coupled plasma–mass spectroscopy (ICP-MS) at Actlabs Ltd. (ANCASTER, Canada). The detection limits for REE, Th, and U were 0.001 μg·L^{-1} in dissolved and total concentration. However, the U dissolved and total concentration in QB-4w was analyzed via inductively coupled plasma–optical emission spectrometry (ICP-OES), with a detection limit of 0.05 mg·L^{-1}.

The soil samples related to the waste rock piles were collected at different heights, since the stockpiles can reach 15 m in height (two soil samples were collected in the top of the pile and two in the slope). Samples (1.5 kg) from each grid were taken with a plastic shovel and transferred to plastic bags. At the laboratory, the samples were air-dried, homogenized, and sieved (fraction < 2 mm). A portion of 200 g of each sample was ground in agate mortars before chemical and mineralogical analysis. The soil pH and oxidation–reduction potential (ORP) were measured in a soil–water solution of a 1:2 ratio using the calibrated electrodes, according to the ASTM D4972 protocol for the determination of pH–H_2O. These measurements were carried out using the PHS-38W Bante instrument. The mineralogical

characterization of the soil and sediment crystalline phases was performed via X-ray diffraction (XRD) using a Bruker D2 Phaser diffractometer equipped with a Cu Kα radiation X-ray tube (monochromatic radiation, λ = 1.5406 Å), operating at 30 kV and 10 mA. Powder diffractograms were obtained in the 4–70° 2θ range, using a 1° divergence slit, scanning at 1° 2θ/min. The mineral identification was carried out according to previous works [28,29], and the mineral proportions were estimated through semi-quantification based on peak areas [30,31], calculated and weighted by empirically estimated factors [32,33]. Given the uncertainties involved in the semi-quantification method, the results obtained should only be taken as rough estimates of the mineral percentages.

The actinide and lanthanide concentrations in soils and sediments were determined at Actlabs Ltd. (ANCASTER, Canada) by the means of Instrumental Neutron Activation Analysis (INAA) and ICP-MS. The detection limits are 0.1 mg/kg for the trace elements (Th, and U), and from 0.05 mg/kg for Eu to 0.1 mg/kg for La, Ce, Pr, Nd, Sm, Gd, Tb, Dy, Ho, Er, Tm, Yb, and Lu. In this work, the REE were divided into three groups, whereby [34]: (a) La through to Nd are considered light rare earth elements (LREEs), (b) Sm to Ho are called middle rare earths (MREEs), and (c) Er through to Lu are named heavy rare earths (HREEs). The Ce and Eu anomalies were determined based on [35].

4. Results

4.1. Water Samples

4.1.1. Physical–Chemical Parameters

The field parameters obtained for the three water samples collected in the Quinta do Bispo old uranium mine, as well as the chemical composition, are shown in Table 1. The pH values of waters range between 5.08 and 7.77, with the more acidic sample in the open pit. The highest Eh, EC, and TDS values also correspond to the open-pit sample (QB-4w). The groundwater collected upstream of the open pit (QB-11w) has the lowest values of EC and TDS.

Table 1. Physical–chemical parameters and dissolved trace element concentrations of the water samples collected inside and outside the Quinta do Bispo old uranium mine (Viseu, Portugal) (TDS, OD are expressed in $mg \cdot L^{-1}$ and trace elements in $\mu g \cdot L^{-1}$; ΣLREE corresponds to the sum of La, Ce, Pr, and Nd dissolved concentrations; ΣMREE are the sum of Sm, Eu, Gd, Tb, Dy, and Ho; ΣHREE are the sum of Er, Tm, Yb, and Lu concentrations); normalized values of PAAS are denoted with the subscript N.

	Inside the Mine Area		*Outside the Mine Area*
	QB-4w **(Open Pit)**	**QB-11w** **(Upstream of the Open Pit)**	**QB-7w** **(Downstream of the Open Pit)**
pH	5.08	7.77	6.31
Eh (V)	0.53	0.35	0.20
OD	9.84	10.7	5.98
EC	954	81.0	276
Temp	16.2	16.2	14.8
TDS	620	52.0	179
U	404	2.73	0.63
Th	0.003	0.009	0.007
La	1.80	0.06	0.04
Ce	4.49	0.07	0.05
Pr	0.66	0.02	0.008
Nd	3.11	0.07	0.043
Sm	0.96	0.03	0.01
Eu	0.58	0.007	0.002
Gd	1.43	0.01	0.02

Table 1. *Cont.*

	Inside the Mine Area		*Outside the Mine Area*
	QB-4w (Open Pit)	**QB-11w (Upstream of the Open Pit)**	**QB-7w (Downstream of the Open Pit)**
Tb	0.29	0.005	0.002
Dy	1.57	0.03	0.01
Ho	0.29	0.006	0.003
Er	0.72	0.02	0.01
Tm	0.09	0.003	0.002
Yb	0.50	0.02	0.02
Lu	0.07	0.002	0.004
Th/U	7.46×10^{-6}	0.003	0.01
(Ce/Ce*)*	0.947	0.54	0.64
(Eu/Eu*)*	2.30	1.81	0.73
(La/Sm)$_N$	0.28	0.36	0.53
(La/Yb)$_N$	0.27	0.24	0.13
ΣLREE	10.1	0.22	0.14
ΣMREE	5.11	0.08	0.05
ΣHREE	1.37	0.04	0.04
ΣREE	16.5	0.34	0.23

$^*\left(Ce/Ce^* \right) = \left[Ce_N / \sqrt{(La_N * Pr_N)} \right]$; $^*\left(Eu/Eu^* \right) = \left[Eu_N / \sqrt{(Sm_N * Gd_N)} \right]$, where $_N$ is the REE values after normalization according to PAAS [35].

4.1.2. Actinide and Lanthanide Behavior

The U, Th and ∑REE dissolved concentrations in the water samples inside the mine area (QB-4w, QB-11w) are between 2.73 and 404, 0.003 and 0.009, 0.03 and 16.5 μg·L^{-1}, respectively (see Table 1). In contrast, the water sample collected downstream of the open pit (QB-7w) has the lowest ∑REE and U dissolved concentration in comparison with the water samples taken inside the mine area. The highest U and REE dissolved concentrations correspond to sample QB-4w (open pit). Regarding the Th/U ratio, lower values have been reported in the water samples collected inside the mine area, while QB-7w has the highest ratio.

The REE patterns of the water samples (dissolved concentration) normalized according to Post-Archean Australian Shale (PAAS) [36] are shown in Figure 2. A general enrichment of the HREE relative to the LREE is observed. The water from the open pit (QB-4w) presents the highest REE contents and a positive Eu anomaly. The groundwater collected upstream of the open pit (QB-11w) shows negative Ce and Gd anomalies. In general, the water collected in the Castelo river (QB-7w), outside the mine area, has the lowest REE contents, a negative Ce anomaly and a slight Gd positive anomaly.

A direct relation between Th dissolved concentration with the pH is observed (Figure 3a), while an inverse relation between U relative to pH seems to occur in the water samples (Figure 3b). In fact, for lower pH values (≈5), observed in sample QB-4w, higher U, ∑LREE, ∑MREE, and ∑HREE dissolved concentrations were observed. The samples with pH values 6–8 have a lower and more stable dissolved concentration of these elements (Figure 3b–e).
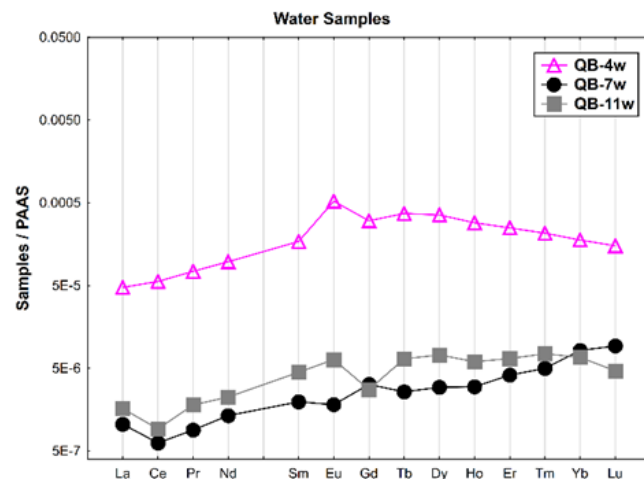
Figure 2. The REE patterns of the water samples from the Quinta do Bispo old uranium mine, Viseu (Portugal) normalized according to PAAS.
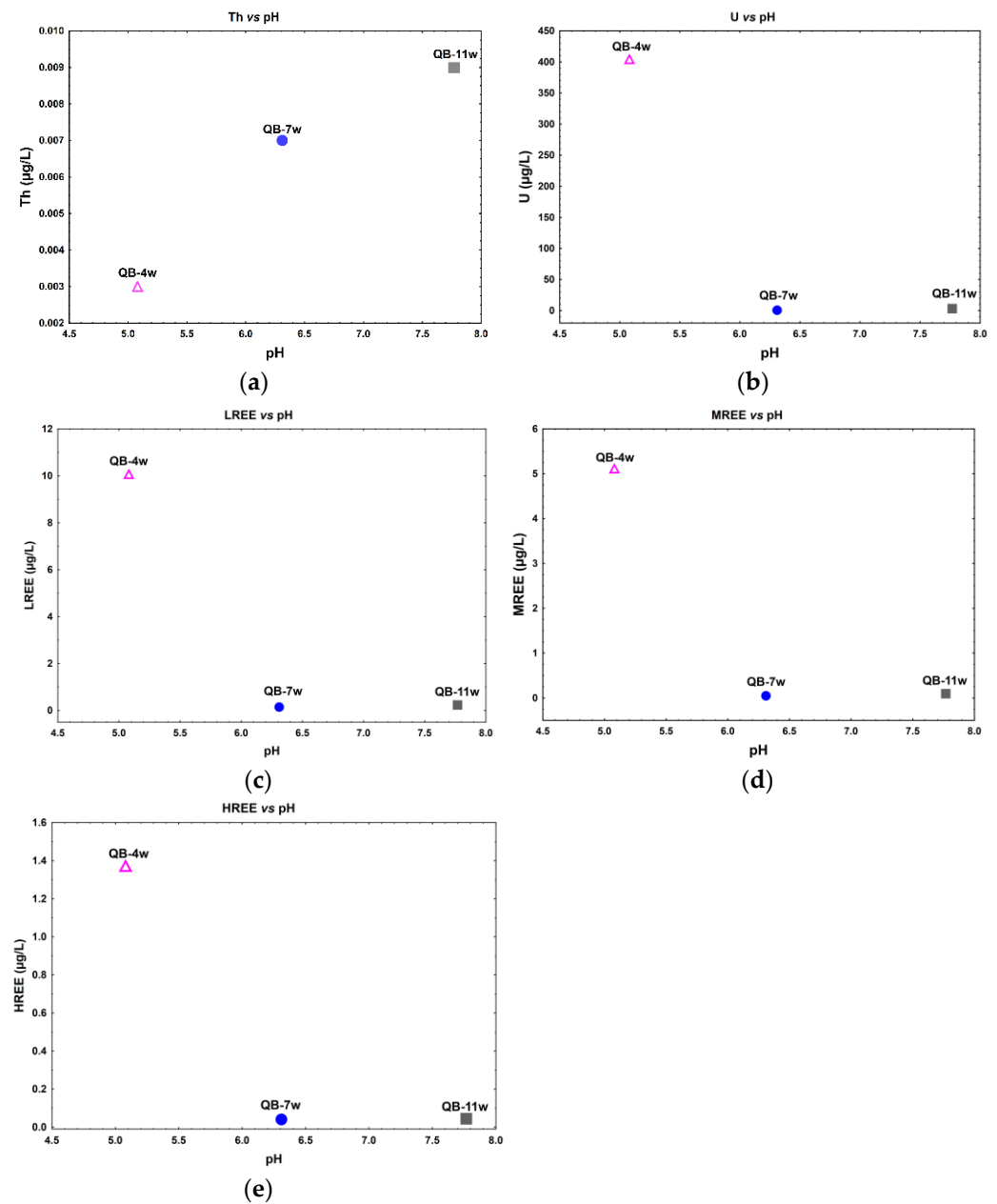
4.2. Soil and Sediment Samples

4.2.1. Physical–Chemical Parameters

The physical–chemical parameters, and the actinide and lanthanide concentrations determined for the soil and sediment samples from the Quinta do Bispo old uranium mine are shown in Table 2.

Table 2. Physical–chemical parameters and trace element concentrations of the soil and sediment samples collected inside and outside the Quinta do Bispo old uranium mine area (Viseu, Portugal) (trace elements are expressed in mg/Kg; n.d. not detected; ∑LREE are the sum of La, Ce, Pr, and Nd concentrations; ∑MREE are the sum of Sm, Eu, Gd, Tb, Dy, Ho; ∑HREE corresponds to the sum Er, Tm, Yb, Lu; normalized values are denoted with the subscript N).

	Soils and Sediments Collected Inside the Mine Area									Soils and Sediments Collected Outside the Mine Area		
	Waste Rocks				**Surrounding the Open Pit**							
Type	**Soil Samples**				**Sediment**	**Soil Samples**				**Sediment**	**Soil Samples**	
	QB-1	**QB-2**	**QB-3**	**QB-10**	**QB-4 SED**	**QB-5**	**QB-6**	**QB-8**	**QB-9**	**QB-7 SED**	**QB-7**	**QB-12**
pH	4.79	5.12	4.58	4.60	8.58	5.61	5.07	5.95	4.22	4.73	4.91	4.94
Eh (V)	0.33	0.32	0.34	0.34	0.16	0.29	0.32	0.28	0.36	0.34	0.33	0.33
U	139	62.1	166	55.4	39.4	13.6	8.30	637	22.2	12.2	17.8	53.7
Th	8.80	19.6	15.9	25.1	17.9	35.3	8.70	10.1	21.2	19.8	7.80	30.4
La	28.1	51.0	52.4	51.1	35.6	58.8	16.7	41.4	47.7	15.8	41.5	60.2
Ce	61.2	103	112	102	75.3	119	37.8	85.5	94.3	33.1	86.0	124
Pr	6.90	11.6	13.0	11.8	8.50	14.0	4.00	10.3	10.6	3.70	9.50	14.0
Nd	27.6	44.6	53.7	44.5	32.6	54.8	15.4	42.5	40.0	13.3	36.0	54.5
Sm	5.30	8.60	9.10	8.20	5.80	9.10	2.80	8.80	6.40	2.60	6.80	10.7
Eu	1.09	0.90	1.80	0.96	0.67	0.86	0.38	2.58	0.86	0.41	0.74	0.85
Gd	4.50	6.60	7.90	6.40	4.80	7.50	2.40	10.4	5.60	2.00	5.10	7.00
Tb	0.60	0.70	0.80	0.70	0.60	0.80	0.30	1.50	0.60	0.20	0.60	0.70
Dy	3.20	3.80	4.00	3.70	3.00	4.80	1.70	9.10	3.30	1.20	3.00	3.80
Ho	0.50	0.70	0.60	0.60	0.50	0.80	0.30	1.60	0.60	0.20	0.50	0.60
Er	1.40	1.50	1.40	1.50	1.30	2.20	0.90	4.00	1.40	0.60	1.30	1.60
Tm	n.d.	n.d.	n.d.	n.d.	n.d.	0.30	n.d.	0.50	n.d.	n.d.	n.d.	n.d.
Yb	1.30	1.40	1.20	1.40	1.30	2.00	0.90	2.90	1.30	0.60	1.20	1.50
Lu	n.d.	n.d.	n.d.	n.d.	n.d.	0.30	n.d.	0.40	n.d.	n.d.	n.d.	n.d.
Th/U	0.06	0.32	0.10	0.45	0.45	2.60	1.05	0.02	0.95	1.62	0.44	0.57
(Ce/Ce*)*	1.01	0.97	0.99	0.95	0.99	0.95	1.06	0.95	0.96	0.99	0.99	0.98
(Eu/Eu*)*	0.98	0.53	0.94	0.58	0.56	0.46	0.65	1.19	0.63	0.55	0.79	0.43
(La/Sm)$_N$	0.78	0.87	0.85	0.92	0.90	0.95	0.88	0.69	1.10	0.90	0.90	0.83
(La/Yb)$_N$	1.59	2.68	3.22	2.69	2.02	2.17	1.37	1.05	2.70	1.94	2.55	2.96
∑REE	142	234	258	233	170	275	83.6	221	213	73.7	192	279
∑LREE	124	210	231	209	152	247	73.9	180	193	65.9	173	253
∑MREE	15.2	21.3	24.2	20.6	15.4	23.9	7.88	34.0	17.4	6.61	16.7	23.7
∑HREE	2.70	2.90	2.60	2.90	2.60	4.80	1.80	7.80	2.70	1.20	2.50	3.10

$^*\left(\text{Ce}/Ce^*\right) = \left[Ce_N/\sqrt{(La_N*Pr_N)}\right]; \,^*\left(\text{Eu}/Eu^*\right) = \left[Eu_N/\sqrt{(Sm_N*Gd_N)}\right]$, where $_N$ is the REE values after normalization according to PAAS [35].

Figure 3. Actinide and lanthanide dissolved concentration in relation to the pH in the water samples from the Quinta do Bispo old uranium mine, Viseu, Portugal. (**a**) Th vs. pH; (**b**) U vs. pH; (**c**) ΣLREE vs. pH; (**d**) ΣMREE vs. pH; and (**e**) ΣHREE vs. pH.

The pH of the soil and sediment suspension for most of the studied samples is acidic, with the exception of the sediment collected inside the open pit (QB-4 SED), which is alkaline (see Table 2). The soil samples collected inside the mine area and taken from the waste rock pile exhibited pH and Eh values between 4.58 and 5.12, and 0.32 and 0.34, respectively. Moreover, the soil samples collected surrounding the open pit (inside the mine area) showed pH and Eh values varying from 4.22 to 5.95, and 0.28 to 0.36, correspondingly. The highest pH value of all the soil samples collected inside the mine area corresponds to QB-8, while the highest Eh value was found in QB-9. Concerning the soil samples collected outside the mine area, the pH and Eh values are similar (around 4.90 and 0.30, respectively). On the other hand, the sediment collected outside the mine area (QB-7 SED) has a lower pH (4.73) and higher Eh (0.34) values when compared with the sediment collected inside the mine area.

4.2.2. Mineralogy

The XRD results enhance the differences on the mineralogical assemblage of the samples according to their nature and location. The identified mineral phases are shown in Table 3 and are placed in the descending order of their proportion in the different samples (from the most to the least abundant). Silicates (quartz, feldspars, plagioclase, phyllosilicates) are the mineral phases common to all samples in varying amounts. Alongside that, a variety of accessory minerals occur. In the soil samples QB-1 and QB-3 from the waste rocks, uranium mineral phases (torbernite, uraninite, fourmarierite, and autunite) and traces of hematite and rutile were also detected. In the soil sample QB-10, traces of alunite were found. The soils surrounding the open pit also reflect the heterogenous mineralogical composition, with the occurrence of traces of calcite in sample QB-6, plumbogummite in QB-5, and torbernite and traces of thorianite (syn) in QB-8.

Table 3. Mineralogical composition of soil and sediment samples collected inside and outside the Quinta do Bispo old uranium mine area (Viseu, Portugal).

Location	Sample	Mineralogical Composition	Sample Type
Soil and sediment samples collected inside the mine area	QB-1	K-feldspars, quartz, plagioclase, phyllosilicates, torbenite, uraninite, hematite	Soils collected in the waste rocks
	QB-2	Quartz, K-feldspars, plagioclase, phyllosilicates	
	QB-3	Quartz, phyllosilicates, autunite, plagioclase, K-feldspars, fourmarierite, rutile	
	QB-10	K-feldspars, quartz, plagioclase, phyllosilicates, alunite	
	QB-4 SED	K-feldspars, quartz, plagioclase, phyllosilicates, calcite	Soils and sediment collected surrounding the mine area
	QB-5	K-feldspars, quartz, phyllosilicates, plagioclase, plumbogummite	
	QB-6	Plagioclase, quartz, K-feldspars, phyllosilicates, calcite	
	QB-8	Quartz, K-feldspars, phyllosilicates, plagioclase, thorianite, torbenite	
	QB-9	Quartz, K-feldspars, plagioclase, phyllosilicates	
Soil and sediment samples collected outside the mine area	QB-7	Quartz, K-feldspars, plagioclase, phyllosilicates	
	QB-12	Quartz, K-feldspars, phyllosilicates, plagioclase	
	QB-7 SED	Quartz, K-feldspars, plagioclase, phyllosilicates, thorogummite	

The two soil samples collected outside the mine area have different geological contexts, one developed in a granitic geological background (QB-12) and the other one in an alluvial context (QB-7). These soil samples have a similar mineralogical composition, mainly comprising quartz, K-feldspars, plagioclase (albite), and phyllosilicates. In addition, the stream sediment QB-7 SED has traces of thorogummite (see Table 3).

4.2.3. Actinide and Lanthanide Behavior

The U and Th concentrations in the soil samples from the waste rock piles inside the mine area (QB-1, QB-2, QB-3, and QB-10) range between 62.1 and 166, and 8.8 and 25.1 mg/kg, respectively. Additionally, the ∑REE concentration in these samples is from 142 to 258 mg/kg. Sample QB-3 has the highest ∑LREE, ∑MREE, and ∑REE, while QB-2

and QB-10 have the highest $\sum$HREE concentration. The Th/U ratio in this group of samples ranges from 0.06 to 0.45, where the lowest values were found in QB-1, while the highest values were reported in QB-10.

Regarding the soils collected surrounding the mine area (QB-5, QB-6, QB-8, and QB-9), their U and Th concentration are between 8.3 and 637, and 8.70 and 35.3 mg/kg, correspondently, where QB-8 has the highest U concentration and QB-6 shows the lowest Th and U concentrations. Furthermore, the $\sum$REE concentration in this group of samples ranges from 83.6 to 275 mg/kg. Although the highest $\sum$REE was found in QB-5, sample QB-8 shows the highest $\sum$MREE and $\sum$HREE concentrations. In addition, the Th/U ratio in these samples is in the range of 0.02 to 2.60, and the highest value corresponds to QB-5. Concerning the sediment from the open pit (QB-4 SED), the U, Th, and $\sum$REE concentrations found (39.4, 17.9, and 170 mg/kg) are similar to ones found for the soil samples collected inside the mine area.

In the samples collected outside the mine area, the soil sample QB-12 has the highest U, Th, and $\sum$REE concentration (see Table 2). The Th/U ratio is between 0.44 and 0.57, of which the highest value corresponds to QB-12. In addition, the sediment sample from outside the mine area (QB-7 SED) exhibits lower U and $\sum$REE concentrations when compared with the sediment collected inside the mine area.

The results obtained for the ratio $(La/Yb)_N$ have a diversity of values inside the mine area, in which the ratios ranged between 1.59 and 3.22 for the soil samples from waste rock piles, and 1.05 and 2.70 for the soils surrounding the open pit. QB-12 exhibits the highest ratio (2.96) in the soil samples collected outside the mine area. Regarding the sediment samples, QB-4 SED has a slightly higher ratio $(La/Yb)_N$ in comparison with QB-7 SED. On the other hand, the result from the ratio $(La/Sm)_N$ did not exhibit a huge variability in the samples. For instance, the highest ratios in the soil samples collected inside (including the waste rock) and outside the mine area were found in QB-9 (1.10) and QB-12 (0.83).

The PAAS-normalized REE profiles of the soil samples from the waste rock piles revealed an overall fractionation pattern in general, with an enrichment of LREE and MREE when compared to the HREE (Figure 4), particularly in sample QB-3 $((La/Yb)_N = 3.22)$. Subgroup 2 of the waste rocks shows a different REE pattern, with negative Eu anomalies $(Eu/Eu^* \approx 0.5)$, which are the typical features of the REE distribution of regional granites, and a similar enrichment of LREE-relative HREE $((La/Yb)_N = 2.7)$.
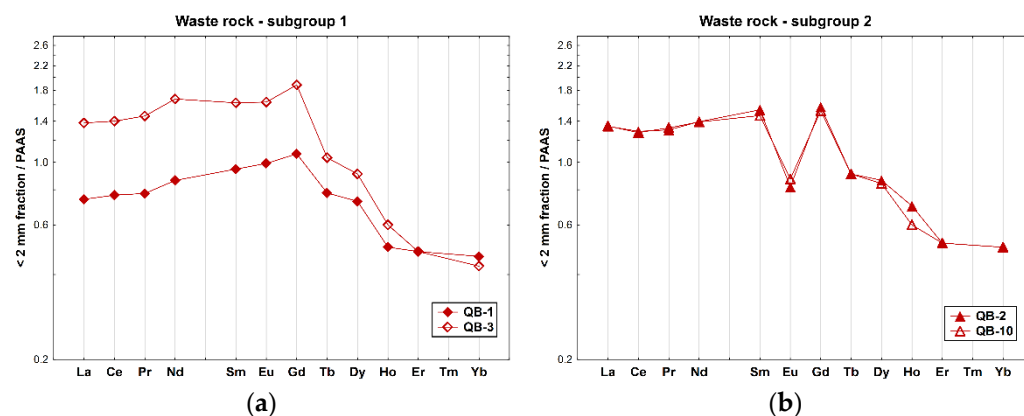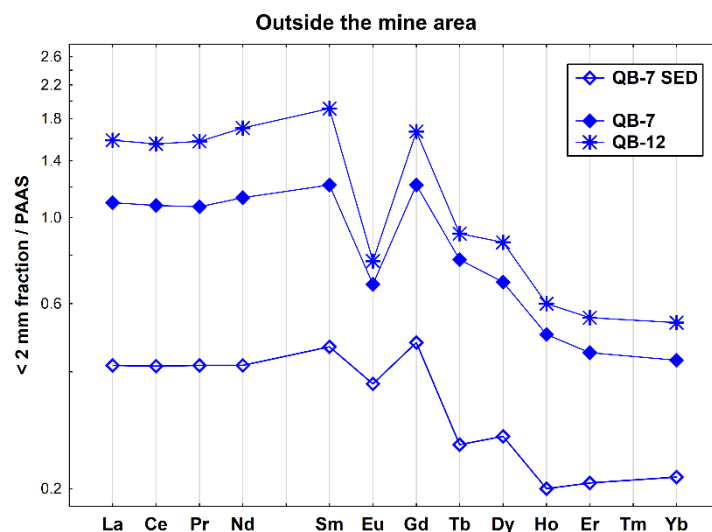

Figure 4. REE patterns of the whole samples of soils collected inside the mine area, on the waste rock piles from the Quinta do Bispo old uranium mine (Viseu, Portugal) relative to PAAS [36]: (**a**) subgroup 1 (QB-1 and QB-3); and (**b**) subgroup 2 (QB-2 and QB-10).

Concerning the samples collected inside the old mine but surrounding the open pit, the REE patterns of the four soil samples and the sediment sample QB-4 SED are given in Figure 5. These samples show negative Eu anomalies $(Eu/Eu^* = 0.46–0.65, \text{average} = 0.58)$, except for QB-8 that has a slight positive Eu anomaly $(Eu/Eu^* = 1.19)$ and an enrichment of MREE relative to LREE $((La/Sm)_N = 0.69)$ and HREE. Moreover, sample QB-6 is depleted in all REEs, has a lower fractionation and a slightly positive Ce anomaly $(Ce/Ce^* = 1.06)$.
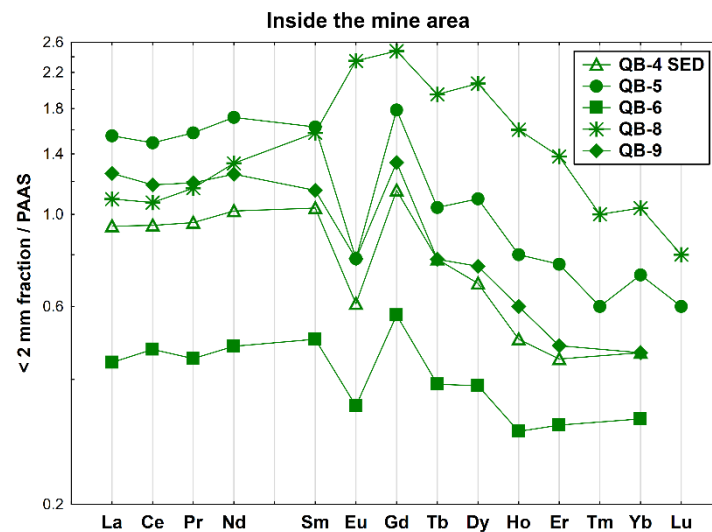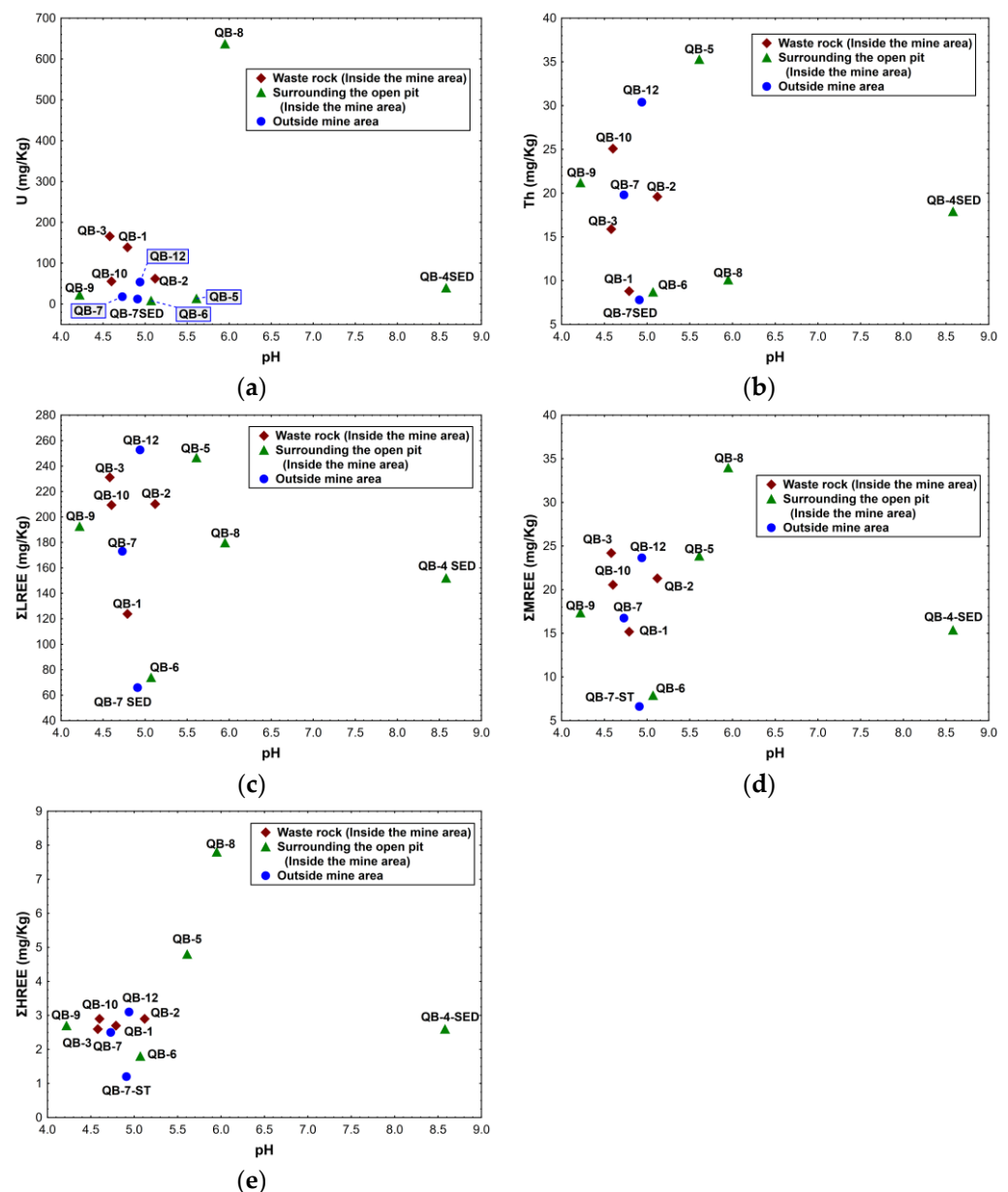
Figure 5. REE patterns of the soil and sediment samples collected inside the Quinta do Bispo old uranium mine, surrounding the open pit (Viseu, Portugal), relative to PAAS.

The REE patterns of the two soils and one stream sediment collected outside the mine area show the typical features of the surrounding granitic geological background, showing a relative enrichment of LREE relative to MREE ($(La/Sm)_N$ = 0.83–0.90) and a strong negative Eu anomaly (Eu/Eu^* = 0.43–0.79) (Figure 6). In addition, the two soil samples have a higher fractionation ($(La/Yb)_N$ = 2.55–2.96), while the stream sediment (QB-7 SED) exhibits the lower fractionation and is depleted in REEs, particularly HREEs.

Figure 6. REE patterns of the soil and stream sediment samples collected outside the Quinta do Bispo old uranium mine (Viseu, Portugal), relative to PAAS.

The chemical results obtained for the soil samples collected inside the mine area on the waste rock piles do not show a clear relationship between U, Th, ΣLREE, ΣMREE, ΣHREE, and pH values. However, in these samples, the one with lowest pH value (QB-3) has the highest ΣLREE and ΣMREE concentrations. In addition, the sample with highest pH value (QB-2) among these shows the lowest U concentration and a higher ΣHREE concentration (Figure 7).

Figure 7. Relation between the chemical composition of the soils and sediments, and the respective pH for the samples collected inside and outside the Quinta do Bispo old uranium mine (Viseu, Portugal): (**a**) U vs. pH; (**b**) Th vs. pH; (**c**) ΣLREE vs. pH; (**d**) ΣMREE vs. pH; (**e**) ΣHREE vs. pH.

In the soil samples collected in the area surrounding the open pit, no relationship between the chemical results and pH values was found (see Figure 7). Nevertheless, sample QB-8 has a higher U, ΣMREE, and ΣHREE concentration and a higher pH value.

Concerning the sediment sample collected inside the mine area (QB-4 SED), this sample has the highest pH value of all the samples taken inside the mine area, but the chemical contents obtained are lower than some soil samples (QB-6 and QB-5).

The soil samples collected outside the mine area (QB-7 and QB-12) exhibit similar pH values, but the lanthanide and actinide concentrations vary significantly. Additionally, the sediment sample taken outside the mine area has lower pH values and lower chemical concentrations in comparison with the other sediment sample (see Figure 7a–e).

When the soil samples are studied considering the pH values and not the location, as described previously, a tendency for higher Th contents with the increase in pH appears to be found in some samples, such as QB-9, QB-10, QB-12, and QB-5, or in QB-3, QB-7, and

QB-2 (see Figure 7b). Regarding the REE, high values of ΣLREE were found for the sample with the highest pH, and samples with similar pH values preserve an analogous chemical behavior despite the location of the samples (Figure 7c). On the other hand, the ΣMREE and ΣHREE (Figure 7d,e) samples with a pH below 6 are gathered and have similar REE contents. The only exception is sample QB-8, where the ΣMREE and ΣHREE concentrations are higher.

5. Discussion

When regarding the studied parameters for the water samples (pH, EC, OD, TDS) in the Castelo river and the groundwater (inside the mine area), the samples are not affected by the open pit, since their physical–chemical conditions are completely different to the ones found for the QB-4w sample. Concerning the relation between Th and U, the water samples have much higher concentrations of U with respect to Th (see Table 1), which is certanly due to the lower mobility of the Th in aqueous media as a result of the pH variation, oxidation–reduction conditions, and the complex formation with inorganic ions such as hydroxide, carbonate, phosphate, and organic matter [37]. In addition, when the thorium is found as thorite ($ThSiO_4$) in sediment samples, its solubility in water is very low [37]. This behavior was also found in this study, which can be explained by the presence of thorogummite (thorite group) in the sediment collected outside the mine area (QB-7 SED).

On the other hand, a strong relation between the REE and U concentrations in the water samples seems to occur. This is very clear in the sample from the open pit (QB-4w), where the U and REE dissolved concentrations are significantly higher when compared to the other two water samples (Figure 3b). This behavior can be related with the lower pH in this sample that enables the dissolution and mobility of metals, which could lead to the formation of more soluble metal ions and increase the activity of the water [38,39]. In addition, the relation between REE and Th dissolved concentration is not clear, which might be due to the lower mobility and solubility of Th in the aqueous system.

Concerning the REE anomalies, the positive Eu anomaly found in the QB-4w sample is in accordance with the respective sediment (QB-4-SED), which shows a negative Eu anomaly, typical of the granitic rocks [40]. Regarding the groundwater sample (QB-11w), the REE pattern is similar to one found around the world, with a negative Ce anomaly and positive Eu anomaly, as already reported [41,42]. The negative Ce anomaly results from the oxidation state of the water and the lower solubility of Ce^{4+} relative to Ce^{3+}, and it depends on the weathering processes, pH, redox conditions, complexing ligands, and hydrogeological factors [42]. The REE pattern of the water from the Castelo river (QB-7w), differs from the groundwater mainly in the Eu anomaly and the slightly higher HREE contents. The river waters have been studied by several authors [42–46], and similar behaviors to the QB-7w were described, confirming the "natural" source of this water, unaffected by the old mine.

Concerning the soil samples, a general enrichment of REE is observed when the values were normalized to PAAS, which might be explained by the weathering conditions that lead to a higher REE mobilization and incorporation in newly formed crystalline or amorphous phases. However, QB-1 (the sample collected in the waste rock pile) and QB-6 (the soil sample collected surrounding the mine area) are depleted in REE relative to the PAAS concentration, which can be due to the REE retention in primary minerals, which is resistant to the weathering processes, as reported is previous studies [47–49].

Regarding the actinides, the variations in the U contents within the soil samples can be due to different U contents of ore-processing residues, or the remobilization and trapping of U within the tailings. However, the U concentration is generally higher than Th in all samples, with the exception of QB-5. Moreover, the variations in U contents are larger than the Th in the soil samples, which might suggest that U was remobilized under the weathering conditions after the deposition of the tailings, but also evidence of the lower mobility of Th during the weathering processes, and its distribution is essentially controlled by the accessory minerals, as mentioned before [48].

In particular, the soil samples collected inside the mine area (including samples from the waste rock piles and surrounding the open pit) have higher U contents and show a relevant diversification of uranium mineral phases (torbernite, uraninite, autunite, and fourmarierite), thus presenting diverse REE signatures, as previously found [50]. The evidence of REE incorporation in uranium oxides, such as uraninite, and a negative Eu anomaly related to the early fractionation of plagioclase was already reported [51–54]. An enrichment of LREE relative to HREE with the REE fractionation, as evidenced by the high $(La/Yb)_N$ and a lower ratio Th/U, was observed in almost all samples, which may be related to the presence of the secondary uranium mineral phases (autunite, torbenite). However, the soil QB-8 (sample collected surrounding the open pit) has the highest MREE and HREE contents, which can be due to diverse factors such as the location of the sample (collected in the old course of an old water line within the mine area, in an intersection of two geological faults) (see Figure 1). This could contribute to the presence of heavy minerals as zircon that cannot be detected easily by XRD, but have been reported by other authors in the study area [23,50]. In addition, QB-5 also implies an enrinchment in LREE relative to HREE, but the high Th/U ratio and a strong negative Eu anomaly (Eu/Eu* = 0.46) can be due to the incorporation of LREE into the plumbogummite, as was evidenced in previous work [55]. Additionally, soil samples with the typical mineralogical composition of igneos rock (QB-2, QB-10, QB-9) and negative Eu anomalies (Eu/Eu* range from 0.53 to 0.63) show REE patterns characteristic of the geological background (granite). In fact, the waste rock piles from the Quinta do Bispo mine have geochemical heterogeinety showing different oxidation states and diferent rock sizes. The diferences found between the soil samples might be explained by the contribution of the different surrounding geological background, in addition to different weathering processes.

Despite their different geological background (QB-7–alluvial; QB-12–medium granite), the soil samples collected outside the mine area (QB-7 and QB-12) show a strong relationship between the mineralogical and chemical composition (actinides and lathinides), as well as the physical–chemical parameters (pH), REE fractionation, and the sligth variability in the Th/U ratio. This behavior can be explained by the influence of the granitic unit into the alluvial unit during its deposition.

The sediments collected outside and inside the mine area show similar REE patterns when normalized to PAAS, and the REE concentration in these sediments is lower in comparison with the sediment collected in Europe [39]. In fact, both samples have a negative Eu anomaly (Eu/Eu* = 0.56) and REE fractionation, described by the $(La/Yb)_N$ values (between 1.94 and 2.02). In addition, QB-4 SED (sediment from the open pit) shows slightly higher REE concentrations and a lower Th/U ratio than QB-7 SED (sediment collected in Castelo River outside the mine), which can be explained by the diversity of the waste rock accumulated in the open pit after the mining activity and the different pH values of both samples, that might enable the formation of minerals such as thorogummite.

6. Conclusions

The water, soil, and sediment samples collected inside (including samples from the waste rock piles and surrounding the open pit) and outside the Quinta do Bispo old uranium mine area show diverse behavior due to the geological background of the area where the samples were collected, their mineralogical phases (uranium and iron oxides, lead, uranium, and iron phosphates), and physical–chemical parameters (pH and Eh), which play an important role in the actinide and lanthanide behavior in this uranium environment.

The samples collected inside the mine area exhibit a heterogeneity of behaviors that could be related with the open-pit extraction and ore-process operation that have been used over time, and the exposure of the geological material to atmospheric conditions. Furthermore, the oxidation reaction of waste rock, followed by water infiltration and percolation, favoring drainage and the transfer of dissolved solutes into the environment, is of major relevance. These factors could have influenced the geochemical behavior of

actinides and lanthanides, and favored processes such as secondary mineral formation and adsorption, reducing the mobility of solutes and promoting internal retention in the soils and sediments. In contrast, the samples collected outside the mine area evidenced the influence of the parental material (mainly granitic rocks) and the stability of the primary minerals, since the chemical contents are in general lower than in the samples collected inside the mine area.

Despite a small number of samples having been collected, the approaches applied in this study of water, soils, and sediments of the Quinta do Bispo mine area contribute to a better knowledge of actinide and lanthanide geochemistry and behavior in uranium mining areas.

Author Contributions: Conceptualization, M.I.D., C.D., E.C. and R.M.; methodology, M.I.D., C.D., D.R. and R.M.; validation, M.I.D., C.D., E.C. and R.M.; investigation, A.C., M.I.D., D.R. and R.M.; resources, A.C., M.I.D., C.D., E.C. and R.M.; writing—original draft preparation, A.C., M.I.D. and R.M.; writing—review and editing, M.I.D., C.D., E.C. and R.M.; visualization, A.C., M.I.D. and R.M.; supervision, M.I.D. and R.M.; project administration, M.I.D., C.D., E.C. and R.M.; funding acquisition, M.I.D. and R.M. All authors have read and agreed to the published version of the manuscript.

Data Availability Statement: Data is contained within the article.

Conflicts of Interest: The authors declare no conflict of interest.

References

1. Dushyantha, N.; Batapola, N.; Ilankoon, I.; Rohitha, S.; Premasiri, R.; Abeysinghe, B.; Dissanayake, K. The story of rare earth elements (REEs): Occurrences, global distribution, genesis, geology, mineralogy, and global production. *Ore Geol. Rev.* **2020**, *122*, 103521. [CrossRef]
2. British Geological Survey. Rare Earth Elements. Available online: https://www2.bgs.ac.uk/mineralsuk/download/mineralProfiles/rare_earth_elements_profile.pdf (accessed on 10 November 2022).
3. U.S. Geological Survey. Mineral Commodity Summaries 2018. Available online: https://pubs.er.usgs.gov/publication/70194932 (accessed on 10 November 2022).
4. Balaram, V. Rare earth elements: A review of applications, occurrence, exploration, analysis, recycling, and environmental impact. *Geosci. Front.* **2019**, *10*, 1285–1303. [CrossRef]
5. Huang, X.; Zhang, G.; Pan, A.; Chen, F.; Zheng, C. Protecting the environment and public health from rare earth mining. *Earths Future* **2016**, *4*, 532–535. [CrossRef]
6. Carvalho, F.P. Mining industry and sustainable development: Time for change. *Food Energy Secur.* **2017**, *6*, 61–77. [CrossRef]
7. Costis, S.; Mueller, K.K.; Blais, J.F.; Royer-Lavallée, A.; Coudert, L.; Neculita, C.M. Review of recent work on the recovery of rare earth elements from secondary sources. In *Natural Resources of Canada Report*; Bibliothèque et Archives Canada: Ottawa, ON, Canada, 2019; 63p, ISBN 978-2-89146-926-5.
8. Costis, S.; Mueller, K.K.; Coudert, L.; Neculita, C.M.; Reynier, N.; Blais, J.F. Recovery potential of rare earth elements from mining and industrial residues: A review and cases studies. *J. Geochem. Explor.* **2021**, *221*, 106699. [CrossRef]
9. Moraes, M.; Murciego, A.; Álvarez-ayuso, E.; Ladeira, A. The role of Al13-polymers in the recovery of rare earth elemens from acid mine drainage through pH neutralization. *Appl. Geochem.* **2020**, *113*, 104466. [CrossRef]
10. Nogueria, E.; Licona, F.; Godoi, L.; Brucha, G. Biological treatment removal of rare earth elements and yttrium (REY) and metals from actual acid mine drainage. *Water Sci. Technol.* **2019**, *80*, 1485–1493. [CrossRef]
11. Carvalho, F.P.; Oliveira, J. Alpha emitters from uranium mining in the environment. *J. Radioanal. Nucl. Chem.* **2007**, *274*, 167–174. [CrossRef]
12. Carvalho, E.; Diamantino, C.; Pinto, R. Environmental Remediation of Abandoned mines in Portugal-Balance of 15 years of Activity and New Perspectives. In Proceedings of International Mine Water Association Symposium 2016, Mining Meets Water-Conflicts and Solutions (IMWA), Leipzig, Germany, 11–15 July 2016; Drebenstedt, C., Paul, M., Eds.; ISBN 9781510827141.
13. Empresa de Desenvolvimento Mineiro (EDM). Inventory of Abandoned Mining Areas. Available online: https://edm.pt/area-ambiental/inventariacao-de-areas-mineiras/ (accessed on 7 September 2022).
14. Cabral, M.M.; Silva, M.M.; Neiva, A.M.; Guimarães, F.M.; Silva, P.B. Uranium minerals from a Portuguese variscan peraluminous granite, its alteration, and related uranium-quartz veins. In *Uranium: Compounds, Isotopes and Applications*; Wolfe, G.H., Ed.; Nova Science: New York, NY, USA, 2009; pp. 287–318.

15. Trindade, M.J.; Prudêncio, M.I.; Burbidge, C.I.; Dias, M.I.; Cardoso, G.; Marques, R.; Rocha, F. Study of an aplite dyke from the Beira uraniferous province in Fornos de Algodres area (Central Portugal): Trace elements distribution and evaluation of natural radionuclides. *Appl. Geochem.* **2014**, *44*, 111–120. [CrossRef]

16. Trindade, M.J.; Dias, M.; Prudêncio, M. Urânio e outros elementos em argilas residuais de doleritos, granitos e aplito-pegmatitos da região de Fornos de Algodres, Beira Alta. In Revista Electrónica de Ciências da Terra Geosciences On-Line Journal, Proceedings of the VIII Congresso Nacional de Geologia, Braga, Portugal, 9–17 July 2010; e-Terra: Braga, Portugal, 2010; Volume 13.

17. Dias, M.I.; Prudêncio, M.I.; Waerenborgh, J.C.; Paiva, M.I.; Marques, R.; Vieira, B.J.; Russo, D.; Lobarinhas, D.; Carvalho, E.; Rosa, C. Evaluation of REE potential in portuguese legacy mines. In E3S Web of Conferences Proceedings of the 16th International Symposium on Water-Rock Interaction (WRI-16) and 13th International Symposium on Applied Isotope Geochemistry (1st IAGC International Conference), Tomsk, Russia, 21–26 July 2019; EDP Sciences: Les Ulis, France, 2009. Abstract Number 06003. [CrossRef]

18. Neiva, A.; Antunes, M.H.; Carvalho, P.; Santos, A.C. Uranium and arsenic contamination in the former Mondego Sul uranium mine area, Central Portugal. *J. Geochem. Explor.* **2016**, *162*, 1–15. [CrossRef]

19. Neves, O.; Matias, M. Focos de poluição na área mineira de Cunha Baixa (Viseu, Portugal). *Caderno Lab. Xeolóxico Laxe Coruña* **2004**, *29*, 187–202.

20. Neves, M.; Figueiredo, V.; Abreu, M. Transfer of U, Al, and Mn in the water-soil-plant (*Solanum tuberosum* L.) system near a former uranium mining area (Cunha Baixa, Portugal) and implications to human health. *Sci. Total Environ.* **2012**, *416*, 156–163. [CrossRef]

21. Ramalho, E.; Carvalho, J.; Barbosa, S.; Monteiro, F. Using geophysical methods to characterize an abandoned uranium mining site, Portugal. *J. Appl. Geophys.* **2009**, *67*, 14–33. [CrossRef]

22. Empresa de Desenvolvimento Mineiro (EDM). Recuperação Ambiental na Área Mineira da Quinta do Bispo-Fase 1. Available online: https://edm.pt/projetos/remediacao-ambiental-na-area-mineira-da-quinta-do-bispo/ (accessed on 20 March 2023).

23. Barbosa, S.; Almeida, J.; Chambel, A. 3D modelling of the transmissivity of granitic rocks surrounding the old Quinta do Bispo mine. *Comun. Geológicas* **2014**, *101*, 959–963.

24. Matos, J.; Costa, C.V. *A região uranífera da Cunha Baixa-Quinta do Bispo. Memórias e Notícias. Publicações do Museu e Laboratório de Mineralogia e Geológico da Universidade de Coimbra e do Centro de Estudos Geológicos*; Universidade de Coimbra: Coimbra, Portugal, 1972; pp. 26–47.

25. Dahlkamp, F.J. *Uranium Deposits of the World: Europe*, 1st ed.; Springer: Berlin/Heidelberg, Germany, 2016; p. 511, ISBN 978-3-540-78553-8.

26. Trindade, S. Modelação de Atributos Hidrogeológicos do Maciço Envolvente a Antiga Área Mineira de Quinta do Bispo. Ph.D. Thesis, Universidade Nova de Lisboa, Lisboa, Portugal, 2012.

27. Pereira, R.; Barbosa, S.; Carvalho, F.P. Uranium mining in Portugal: A review of the environmental legacies of the largest mines and environmental and human health impacts. *Environ. Geochem. Health* **2014**, *36*, 285–301. [CrossRef]

28. Brindley, G.W.; Brown, G. *Crystal Structures of Clay Minerals, and Their X-ray Identification*; Mineralogical Society of Great Britain and Ireland: London, UK, 1980; ISSN 0144-1485.

29. ICDD. *Mineral Powder Diffraction File Databook*; International Center for Diffraction Data (ICDD): Newtown Square, PA, USA, 1993.

30. Schultz, L.G. Quantitative interpretation of mineralogical composition X-ray and chemical data for the Pierre Shale. *Geol. Surv.* **1964**, 391. [CrossRef]

31. Rocha, F.T. Argilas Aplicadas a Estudos Litoestratigráficos e Paleoambientais na Bacia Sedimentar de Aveiro. Ph.D. Thesis, University of Aveiro, Aveiro, Portugal, 1993.

32. Galhano, C.; Rocha, F.; Gomes, C. Geostatistical analysis of the influence of textural, mineralogical and geochemical parameters on the geotechnical behavior of the "Argilas de Aveiro" formation (Portugal). *Clay Miner.* **1999**, *34*, 109–116. [CrossRef]

33. Oliveira, A.; Rocha, F.; Rodrigues, A.; Jouanneau, J.; Dias, A.; Weber, O.; Gomes, C. Clay minerals from the sedimentary cover from the Northwest Iberian shelf. *Prog. Oceanogr.* **2002**, *52*, 233–247. [CrossRef]

34. Henderson, P. *Rare Earth Element Geochemistry*, 1st ed.; Elservier Science Publishers: Amsterdam, The Netherlands, 1983; ISBN 9781483289779.

35. Worral, F.; Pearson, D.G. Water-rock interaction in an acid mine discharge as indicated by rare earth element patterns. *Geochim. Cosmochim. Acta* **2001**, *65*, 3027–3040. [CrossRef]

36. Nance, W.B.; Taylor, S.R. Rare earth element patterns and crustal evolution-I. Australian post-Archean Sedimentary rocks. *Geochim. Cosmochim. Acta* **1976**, *40*, 1539–1551. [CrossRef]

37. Langmuir, D.; Herman, J.S. The mobility of thorium in natural waters at lower temperatures. *Geochem. Cosmochim. Acta* **1980**, *44*, 1753–1766. [CrossRef]

38. Nriagu, J.O.; Pacyna, J.M. Quantitative assessment of worldwide contamination of air, water, and soils by trace metals. *Nature* **1998**, *24*, 869–876. [CrossRef]

39. Nordstrom, D.K.; Alpers, C.N. Geochemistry of acid mine waters. In *The Environmental Geochemistry of Mineral Deposits*; Plumlee, G.S., Logsdon, M.J., Eds.; Society of Economic Geologists: Littleton, CO, USA, 1999; Volume 6A, pp. 133–160, ISBN 978-1629490137.

40. Johannesson, K.H.; Cortés, A.; Ramos Leal, J.A.; Ramírez, A.G.; Durazo, J. Geochemistry of Rare Earth Elements in Groundwaters from a Rhyolite Aquifer, Central México. In *Rare Earth Elements in Groundwater Flow Systems*; Johannesson, K.H., Ed.; Water Science and Technology Library: Springer: Dordrecht, The Netherlands, 2005; Volume 51, pp. 187–222. [CrossRef]

41. Migaszewski, Z.M.; Galuszka, A. The Characteristics, Occurrence, and Geochemical Behavior of Rare Earth Elements in the Environment: A Review. *Crit. Rev. Environ. Sci. Technol.* **2015**, *45*, 429–471. [CrossRef]

42. Dia, A.; Gruau, G.; Olivié-Lauquet, G.; Riou, C.; Molénat, J.; Curmi, P. The distribution of rare earth elements in groundwaters: Assessing the role of source-rock composition, redox changes and colloidal particles. *Geochim. Cosmochim. Acta* **2000**, *64*, 4131–4151. [CrossRef]

43. Braun, J.J.; Pagel, M.; Muller, J.P.; Bilong, P.; Michard, A.; Guillet, B. Cerium anomalies in lateritic profiles. *Geochim. Cosmochim. Acta* **1999**, *54*, 781–795. [CrossRef]

44. De Baar, H.; Bacon, M.P.; Brewer, P.G.; Bruland, K.W. Rare earth elements in the Pacific and Atlantic Oceans. *Geochim. Cosmochim. Acta* **1985**, *49*, 1943–1959. [CrossRef]

45. Leleyter, L.; Probst, J.; Depetris, P.; Haida, S.; Mortatti, J.; Rouault, R.; Samuel, J. REE distribution patterns in river sediments: Partitioning into residual and labile fractions. *Comptes Rendus L'académie Sci.-Ser. IIA-Earth Planet. Sci.* **1999**, *329*, 45–52. [CrossRef]

46. Goldstein, S.J.; Jacobsen, S.B. Rare earth elements in river waters. *Earth Planet Sci. Lett.* **1988**, *89*, 35–47. [CrossRef]

47. Nesbitt, H. Mobility and fractionation of rare earth elements during weathering of a granodiorite. *Nature* **1979**, *279*, 206–210. [CrossRef]

48. Braun, J.; Pagel, M.; Herbilln, A.; Rosin, C. Mobilization and redistribution of REEs and thorium in a syenitic lateritic profile: A mass balance study. *Geochim. Cosmochim. Acta* **1993**, *57*, 4419–4434. [CrossRef]

49. Zhiwei, B.; Zhenhua, Z. Geochemistry of mineralization with exchangeable REY in the weathering crusts of granitic rocks in South China. *Ore Geol. Rev.* **2008**, *33*, 519–535. [CrossRef]

50. Wenrich, K.; Cuney, M.; Lach, P. Rare earth elements in uraninite: Breccia pipe uranium district, northern Arizona, USA. In Proceedings of the International Symposium on Uranium Raw Material for the Nuclear Fuel Cycle: Exploration, Mining, Production, Supply and Demand, Economics and Environmental Issues (URAM-2018), Vienna, Austria, 25–29 June 2018; IAEA: Vienna, Austria, 2020; ISBN 978-92-0-130720-0.

51. Mercadier, J.; Cuney, M.; Lach, P.; Boiron, M.-C.; Bonhoure, J.; Richard, A.; Leisen, M.; Kister, P. Origin of uranium deposits revealed by their rare earth element signature. *Terra Nova* **2011**, *23*, 264–269. [CrossRef]

52. Göb, S.; Gühring, J.-E.; Bau, M.; Markl, G. Remobilization of U and REE and the formation of secondary minerals in oxidized deposits. *Am. Mineral.* **2014**, *98*, 530–548. [CrossRef]

53. Aubert, D.; Stille, P.; Probst, A. REE fractionation during granite weathering and removal by waters and suspended loads: Sr and Nd isotopic evidence. *Geochim. Cosmochim. Acta* **2001**, *65*, 387–406. [CrossRef]

54. Pagel, M. The mineralogy and geochemistry of uranium, thorium, and rare-earth elements in two radioactive granites of the Voges, France. *Mineral. Mag.* **1982**, *46*, 149–161. [CrossRef]

55. Bain, D. Plumbogummite-group minerals from Mull and Morvern. *Mineral. Mag.* **1970**, *37*, 934–938. [CrossRef]